Thermodynamic measurements of the first layer of Ne adsorbed on closed-end single-walled carbon nanotube bundles

S. Ramachandran and O. E. Vilches*
Department of Physics, University of Washington, P.O. Box 351560, Seattle, Washington 98195-1560, USA
(Received 2 May 2007; published 6 August 2007)

We report the results of thermodynamic measurements done on Ne films adsorbed on HiPCo™ single-walled, closed-end, purified carbon nanotube bundles. The heat capacity was measured for 17 coverages between 0.015 and 1.14 single atomic layers for 1.8 K$<T<$19 K. A few complementary adsorption isotherms were measured on the same cell over a similar range of coverages for 18.1 K$<T<$29.5 K. Our results indicate that Ne deposits, in order, in high binding energy sites, the grooves on the outside of the bundles, the surface of the outer nanotubes, and after compressing the full monolayer, on a second layer. All of the films show solidlike behavior in the range studied. For the lowest coverage films, we compare our results to theoretical estimates and calculate the one-dimensional Debye temperature. For the higher coverage films, we calculate two-dimensional Debye temperatures and compare to results obtained on Ne adsorbed on flat graphite (Grafoil™). We estimate the two-dimensional (2D) compressibility of the films near monolayer completion from the vapor pressure isotherms. Agreement is found between the monolayer completion coverage inferred from heat-capacity isotherms and a minimum in the compressibility. In spite of the solidlike behavior and similarities to Ne/graphite, we do not observe any phase transition in the range of temperatures and coverages studied, which overlaps with the sublimation, melting, and vaporization transitions of 2D Ne.

DOI: 10.1103/PhysRevB.76.075404 PACS number(s): 65.80.+n, 68.43.−h, 68.65.−k, 65.40.Ba

I. INTRODUCTION

The first atomic layer of simple atoms (molecules) adsorbed on basal plane graphite has been studied extensively.[1] From the large number of thermodynamic, structural, and spectroscopic measurements done in the past 40 years,[2–9] quasi-two-dimensional surface-density–temperature phase diagrams have emerged. Phases observed include gaseous, fluid, and commensurate and incommensurate solids of different types. Continuous and first order phase transitions have been observed, and several two-dimensional (2D) critical exponents have been measured.

Single-walled carbon nanotube bundles (SWNTBs) are particularly interesting substrates for physisorption due to their obvious relationship to a single layer of basal plane graphite (graphene) and the possibility of making quasi-one-dimensional matter. Bundles of a few to hundreds of nanotubes are formed by many parallel tubes of around 1 nm or higher diameter. Even when the nanotubes are closed at the ends, adsorption may be possible in long interstitial sites formed by three or more nanotubes[10] in the interior of the bundle (if these interstices are large enough), on grooves formed by two adjacent nanotubes on the outside of a bundle, and on the curved surface of nanotubes on the outside of the bundle.[11] For single-walled nanotubes, these outside surfaces are "curved graphene." If adsorption in interstitial channels is not possible, adsorption on the outside grooves and on the outside surface of individual nanotubes is expected to proceed in three steps: (a) adsorption of one line of atoms on grooves, (b) adsorption of two additional lines of atoms anchored by the first line of atoms (a so-called three-line phase), and (c) adsorption on the curved graphene. Thus, in principle, one could study unique adsorbed quasi-one-dimensional "lines of atoms" in the grooves, quasi-2D behavior on the outside surface of the bundles to compare to adsorption on graphite, and look for one-dimensional (1D) to 2D [and even three-dimensional (3D)] crossover phenomena.

It is well known that long range order and two-phase coexistence are not possible in infinite 1D matter for $T>0$ K.[12–14] One would not expect to observe any phase transition if very long 1D chains of atoms are formed on the SWNTB, but the physical behavior of finite, relatively short 1D chains is not known but has been partially explored.[15] Furthermore, the thermodynamic behavior of quasi-2D matter formed on the bundles consisting of a few parallel long lines of atoms anchored by atoms deposited on grooves (in our case) 1.4 nm apart is not known. Progress has been made in the study of physisorbed films on SWNTB, both theoretically and experimentally. Reviews of early theoretical developments by Calbi *et al.*[16] and of much of the experimental work by Talapatra *et al.*[17,18] are available.

In this paper, we report the results of a comprehensive thermodynamic study of the adsorption of Ne on HiPCo™ SWNTB using dc calorimetry, complemented by a set of volumetric adsorption isotherms on the same sample cell. Both the amount of Ne adsorbed and the magnitude of the specific heat have been measured accurately. We have explored the entire first layer and beginning of the second layer, measuring heat capacity as a function of temperature between 1.9 and 19 K for essentially constant coverages between 0.015 (2 scc) to 1.14 (153 scc) monolayers and adsorption isotherms above 18 K from 3.1 to 188 scc. We identify four regions for adsorption on SWNTB with increasing coverage: imperfect sites, one line and/or three lines, quasi-two-dimensions, and beginning of the second layer. We calculate the isosteric heat of adsorption, 1D and 2D Debye temperatures, and isothermal compressibility. The 2D regime has a remarkable similarity to the behavior of Ne/graphite, except for the absence of phase transitions.

The reasons for choosing Ne are explained in Sec. II. The rest of the paper is organized as follows: a brief description

of our experimental setup (Sec. III), results (Sec. IV), analysis and discussion of the results (Sec. V), and a brief summary and conclusions (Sec. VI).

II. MOTIVATION

The first layer of Ne/graphite is particularly interesting. This system was the first one where a 2D solid-liquid-vapor triple point was clearly measured by an almost delta-function melting signal in the specific heat (C/Nk) at 13.5 K rising to over 50 from values 20 times smaller within half a degree Kelvin of the triple point.[19] Rapp *et al.*[20] also measured the heat capacity of Ne adsorbed on Grafoil. They confirmed the existence of the triple point melting at 13.5 K and identified a maximum at 15.8 K as the liquid-vapor critical point. Later on, Pengra and Dash[21] measured again the heat capacity of a few coverages of Ne below half a monolayer using a much better quality of exfoliated graphite than the one used in previous studies. They investigated the contribution to the observed triple point melting heat-capacity signal due to edge melting of 2D solid patches. Tibby *et al.*[22] did an extensive measurement of the lattice parameter of Ne/graphite over most of the first solid layer and the beginning of the second layer between 1.5 and 27 K. They found that at 1.5 K and fractional coverages up to at least 0.44 monolayer, the Ne-Ne distance was 3.25 Å, consistent with Ne forming a $(\sqrt{7}\times\sqrt{7})R19°$ commensurate structure, which became incommensurate at higher fractional coverages. This commensurate structure did not exist in scans taken above 7 K. They also measured the lattice parameter of the incommensurate solid at the triple point and along the sublimation and melting line of the incommensurate solid. They found that at the sublimation line and 1.5 K, the Ne-Ne distance was 3.24 Å, while at the monolayer completion, it was 3.115 Å, corresponding to a surface density of 0.119 $Å^{-2}$. Calisti *et al.*,[23,24] using low energy electron diffraction, measured the solid lattice parameters at densities higher than the melting line of 2D Ne adsorbed on single crystal graphite and determined the orientation of the incommensurate solid with respect to the graphite basal plane lattice. They found an agreement with the measurements of Wiechert *et al.* in their range of temperatures studied (at 10 K and between 14.3 and 17.9 K), but the rotation of the monolayer was inconsistent with a commensurate layer albeit at much higher temperature. At monolayer completion and 14 K, they measured 3.09 Å for the Ne-Ne distance, which corresponds to 0.121 $Å^{-2}$ density. The commensurate-incommensurate transition observed in diffraction measurements was not observed by Huff in his earlier calorimetric measurements on Ne/graphite, although the data in this temperature range are sparse. In summary, Ne/graphite has a relatively simple 2D phase diagram similar to what is expected for a van der Waals system, with solid-liquid-vapor triple point and liquid-vapor critical line at temperatures easily measured by calorimetry, which in reduced dimensionality give $T_{T(2D)}\approx 0.55\ T_{T(3D)}$ and $T_{C(2D)}\approx 0.35\ T_{C(3D)}$. This makes Ne an ideal system to study 1D effects and variations in 2D behavior on a graphite-related surface.

Stan *et al.*,[11] using a classical statistical approach, determined the criteria, in terms of Lennard-Jones parameters, for a gas to be imbibed in the interstices and inside the nanotube. They concluded that neon with $\epsilon_{gg}=35.6$ K and $\sigma_{gg}=2.75$ Å is a suitable candidate for adsorption into either site. Theoretical calculations by Calbi and Cole[25] predict the binding energy of Ne on first layer groove sites of carbon nanotube bundle to be 1.5 times that on graphite (30.1 meV).[26] Simulations by Gordillo *et al.*[27] using path integral Monte Carlo methods have estimated the chemical potential of Ne atoms in the interstices and the grooves. They conclude that it is favorable for the Ne atoms to adsorb first in the interstitial channels of (10,10) closed-end carbon nanotubes, where the calculated binding energy is on the order of 1000 K, followed by occupation of the grooves where the calculated binding energy at $T=0$ K is $\approx$659 K. Hence, they state that at temperatures on the order of 40 K, Ne would be incorporated in the interstices of (10,10) and in the interior of open (5,5) carbon nanotubes and is favored to the 1D line phase or the three-line phase on the grooves. Calbi and Riccardo[28] specifically investigated the possibility of H_2 uptake in the interstices of (10,10) bundles and found a high binding site followed by a significant energy barrier at the entrance to the interstices. If this were to occur for Ne, this "plug" could prevent, within a reasonable finite time, adsorption in the interstitial channels.

Kostov *et al.*[29] have calculated the phonon specific heat for Ne adsorbed as one line of atoms on the groove between two ideal nanotubes of 1.38 nm diameter, 1.7 nm apart for two Ne-Ne distances, 3.08 Å (which they call the equilibrium distance) and 2.92 Å (compressed Ne). They found that below about 6 K, a longitudinal mode in the direction of the groove dominates, which produces a low T linear specific heat. Above this temperature, excitations transverse to the groove come into play and eventually dominate, converting the line of atoms into a 3D system with specific heat approaching $C/Nk\approx 2.8$ at about 60 K. Thus, this model yields 1D to 3D crossover properties that one would expect to find in the experimental system. We note though that the 3.08 Å equilibrium distance is already compressed when compared to the Ne-Ne equilibrium 2D solid distance at 1.5 K of 3.21–3.24 Å (Refs. 22–24) or the 3D solid distance below 4 K of 3.16 Å. In quasi-one-dimension, as these lines should behave, zero point motion and only two nearest neighbors could make the Ne-Ne separation even larger than on graphite.

Talapatra *et al.* measured vapor pressure isotherms of Ne, CH_4, and Xe on closed-end nanotube bundles obtained from two sources, Journet *et al.*[30] and CarboLex,[31] and compared the measured to calculated Ne monolayer capacity assuming both scenarios—Ne occupying or not occupying the interstices. These SWNTBs had tube diameter of $\approx$1.4 nm and tube spacing of 1.7 ± 0.1 nm in the bundle.[32,33] From an adsorption isotherm at 22 K on the CarboLex sample, Talapatra *et al.* showed that Ne does not occupy the interstices but occupies the grooves with measured binding energy of 52 meV or 602 K,[17] about 59% larger than the corresponding values on planar graphite. In a later study, Talapatra *et al.*[18] used the same nanotubes produced by Journet *et al.* cited above to measure adsorption isotherms of Ne, CH_4, and

Xe past monolayer completion. Adsorption isotherms for Ne into the second layer between 23.6 and 29.3 K were shown to reveal a small step past monolayer completion. This step was interpreted to be a 1D phase forming on the second layer groove. Adsorption of Ne and other gases on HiPCo™ nanotubes, similar to what we have used in this study, has been only recently carried out[34] by Krungleviciute *et al.* This study looks closely at the second layer adsorption in order to look for more evidence for a 1D phase on the second layer groove. Thus, the available experimental data at this time for Ne/SWNTB have been obtained at temperature high enough to measure its vapor pressure, well above the region where all the phase transitions occur in 2D Ne/graphite.

Of specific relevance to this work, Lasjaunias *et al.*[35] measured the heat capacity of ^{4}He adsorbed on two different types of compressed SWNTBs between 100 mK and 6 K using dc calorimetry. The compressed SWNTB sample was open to the dilution refrigerator vacuum, so the amount of ^{4}He adsorbed had to be estimated. The authors concluded that at very low dosing, a 1D gas was formed with $C/Nk \approx 0.5$ at $T > 2$ K. At low T though, the adsorbed helium film shows specific heat vs temperature behavior that conforms to an Einstein oscillator model. For their highest coverage, perhaps at or above a monolayer, they found that the specific heat had T^2 behavior at low T and $C/Nk \approx 2$ at the highest temperature. In our laboratory, we have measured the heat capacities of ^{4}He and H_2 on HiPCo nanotubes using ac calorimetry.[36] These measurements confirmed the T^2 behavior of the heat capacity for both substances near monolayer completion, with the same magnitude ratio at equal coverages as for adsorption on graphite. The magnitude of the measured heat capacity, though, was not accurate due to long internal equilibration times of the closed calorimeter cell, so 2D Debye temperatures could not be calculated.

III. EXPERIMENT

A cylindrical cell was constructed with oxygen-free high-conductivity (OFHC) copper with inner diameter of 2.22 cm and depth of 0.79 cm; 0.413 g of unbaked HiPCo™ carbon nanotube bundles was packed in the cell. The nanotubes are 97% pure and contain about 3% Fe as impurity. The mean diameter of the nanotubes is 1.1 nm with a full width at half maximum of 0.1 nm. The average spacing between nanotubes in our bundle is about 1.4 ± 0.2 nm.[37] A lid, also made of OFHC copper, with a gas port was then soft soldered to the open end of the cylindrical cup. While soft soldering, the cap was pressed on and the nanotubes were compacted. The density of the packed bed is estimated at 0.25 g/cm^3. The total mass of the copper cell, excluding the nanotubes, is $\approx$11.90 g. The gas port of the cell was attached to the gas feed line with a Kovar-Glass tubing, which also serves as a thermal link to the cryostat. The cell was evacuated down to below 10^{-6} torr for 48 h at over 70 °C before the cell heater and temperature sensors were attached using varnish. A Manganin heater (total resistance of 382 Ω at room temperature) was wound into a "flat coil" and attached to the bottom of the cell with GE7031 varnish and a thin layer of Emerson and Cuming Stycast 1266 epoxy. An uncalibrated Cernox CX1050SD thermistor from Lakeshore was attached to the face opposite to the heater. The Cernox sensor was calibrated against a calibrated (1–6 K) Lakeshore GR-200-50A germanium sensor located on the sample cell between 1.7 and 4 K and for $T > 4$ K, against a calibrated (4–40 K) Lakeshore GR-200-1500A, located on the inner can that also defines the background temperature. The germanium sensor placed on the cell was removed after calibration in order to not add to the heat capacity of the cell.

The dc heat capacity (C) was measured using

$$C = \dot{Q} * \Delta t_{heat} / \Delta T_{max}, \tag{1}$$

where $\dot{Q}$ is the power delivered by the heater, Δt_{heat} is the heating interval, and $\Delta T_{max} = T_f - T_i$ is the difference between the final and initial temperatures calculated at the middle of the heating interval. The process of heat-capacity measurement was automated using National Instrument's LabView Express VII.

The background heat capacity was measured between 1.9 and 19 K. We used research grade Ne from Alphagaz, Long Beach, CA. The actual monolayer capacity of this cell is $\approx$135 scc Ne, as described in the next paragraph. For dosing below 75 scc, the cell was heated to over 40 K before admitting the gas. For coverage greater than 75 scc, dosing was carried out at 25 K. A fill-line heater kept the Ne gas from solidifying in that part of the fill line that goes through the liquid helium bath inside a vacuum jacket. The gas was admitted slowly into the cell, typically over 10 h, by throttling the supply valve. This kept the dosing pressure below the vapor pressure of Ne at the temperature of the fill line. The high temperature dosing served to anneal different coverages.

Several partial volumetric adsorption isotherms of Ne were measured on the same calorimeter cell over the relatively small range of equilibrium pressures covered by a 10 torr Baratron. Pressure isotherms were obtained over a temperature range of 18.1–29.5 K. We started the isotherms at the highest temperature to assure annealing of the sample. After dosing a known quantity of gas and allowing the system to attain equilibrium, we decreased the temperature at constant coverage until the pressure was too low to measure or the system would not attain equilibrium in a reasonable time (several hours). We then dosed a known quantity of gas, at higher temperature if necessary, and repeated the procedure. We were able to reset the temperature to within 0.1 K. The complete set of isotherms covered the range 3.1 scc $< V_{ads} <$ 188 scc. Isotherms obtained at 19.2 and 27.2 K are shown in Fig. 1. The isotherm at 19.2 K gives a monolayer capacity of 135 scc using the point-B method.[38] It is interesting to note that the isotherm at 27.2 K shows apparently decreased monolayer capacity, partly an artifact of being at a much lower ratio of P/P_0, where P_0 is the 3D vapor pressure at a given temperature T. This reinforces the criteria used by Krungleviciute *et al.*[34] of measuring isotherms of different adsorbates and/or substrates at a temperature that is a fixed fraction of the bulk triple point.

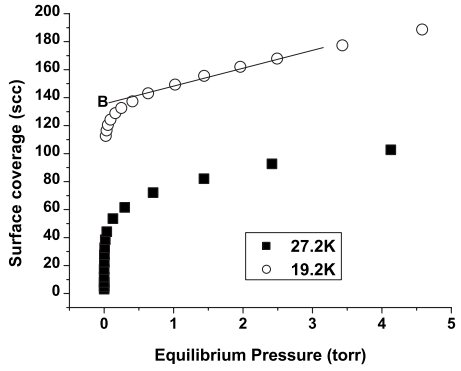

FIG. 1. Pressure isotherm for Ne adsorbed on SWNTB. Point B is indicated in bold.

IV. RESULTS

Figure 2 shows the background heat capacity and the total heat capacity (background plus adsorbate) for the smallest dose of Ne, 1.99 scc. The background heat capacity was fitted to a sixth order polynomial. The fitted polynomial was subtracted from the total heat capacity with adsorbate to extract the heat capacity of the adsorbed film.

Figure 3 shows the difference heat capacity for the measurement shown in Fig. 2, as well as for adsorbate doses of 3.98, 5.98, and 11.91 scc. The data are grouped into "low coverage," Fig. 3, where the film progression is close to the predicted one-line phase, the three-line phase, Fig. 4, and "high coverage," Fig. 5, where the neon atoms occupy all the sites above plus the curved surface of the carbon nanotubes. As stated above, monolayer completion occurs at ≈135 scc.

It may be noted from the figures that the heat capacity increases rapidly at low temperatures. The rate of increase gets smaller close to 12 K, and the heat capacity reaches a plateau above 15 K.

From the C vs T data, heat-capacity isotherms were constructed. Figure 6 shows three such isotherms with all the coverages studied. Points of inflection are seen for Ne coverage between 64 scc (at 10 K) to 66 scc (at 4 K), shown with a downward arrow.

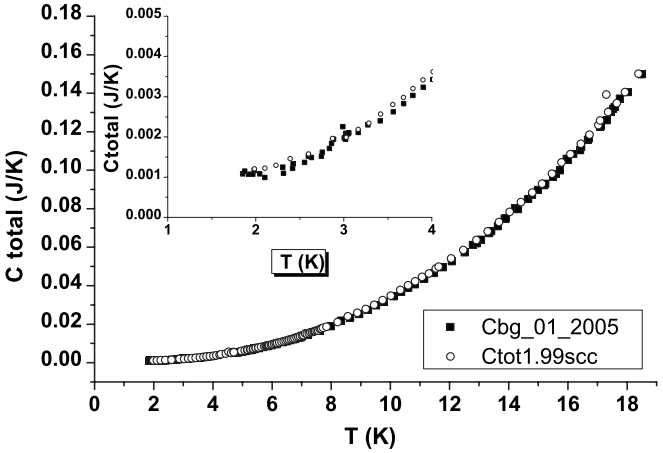

FIG. 2. Background heat capacity (filled squared) and background plus 1.99 scc STP Ne adsorbed (open circles) vs T. Inset shows the lowest T data in an expanded scale.

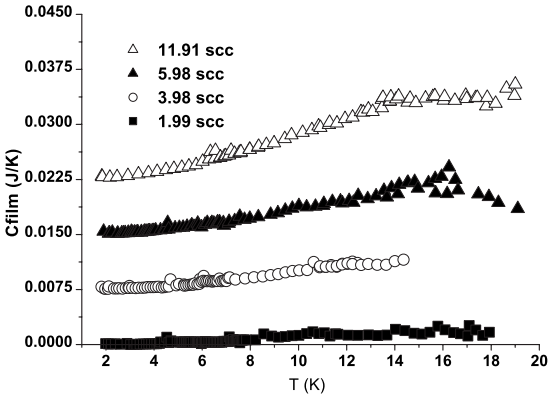

FIG. 3. C vs T of Ne films at several low coverages where the film is expected to be 1D. Each curve is offset by 0.0075 J/K for clarity.

Measurements in our laboratory of the ac heat capacity of H_2 and ^{4}He on a smaller cell (mass of nanotubes is 0.106 g) with identical nanotubes[36] show more pronounced inflections in the heat-capacity isotherms at 0.38 and 0.35 of a monolayer, respectively. When compared with the results of ^{4}He neutron diffraction results of Pearce *et al.*,[37] these inflections correspond approximately to the completion of the three lines of atoms on the grooves. An inflection is also seen in Fig. 6 between 130 scc (at 10 K) and 140 scc (at 4 K) indicated by an upward arrow, marked "M." This point of inflection is due to the completion of the monolayer and agrees closely with the monolayer capacity of 135 scc determined from the adsorption isotherms.

At all coverages, and especially at the higher ones, as the heat capacity was being measured, the 3D gas pressure was recorded in order to estimate the desorption contribution to the heat capacity. The highest coverages measured showed a significant contribution (as high as 5% of the film heat capacity and increasing with an increase in temperature) above 15 K. The data shown have this contribution subtracted. On the other hand, the ratio of Ne molecules in the 3D gas phase to what is on the surface of the nanotube is ≈3000 ppm at

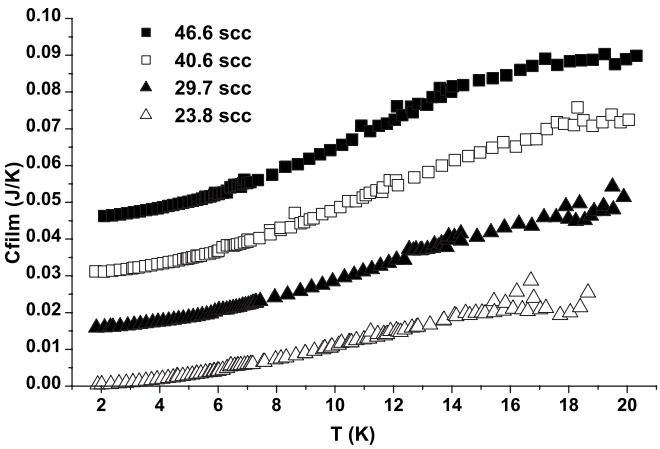

FIG. 4. C vs T of Ne films at few coverages within the single-line phase and into the three-line phase. Each curve is offset from the one below by 0.015 J/K.

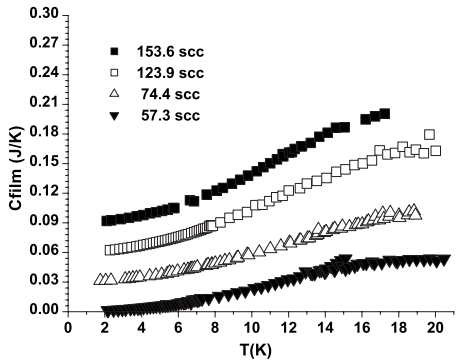

FIG. 5. C vs T at several Ne coverages from filling of the grooves into the second layer. Each curve is offset by 0.03 J/K.

18 K for 1.3 monolayer coverage and about 36 ppm at 20 K for 0.5 monolayer coverage. Thus, the surface coverage is essentially equal to the total quantity of Ne dosed.

Specific heat isotherms for various coverages are shown in Fig. 7. For all coverages, the specific heat exceeds a value of 2 above 15 K. In Fig. 8, the specific heat is shown only up to 34.6 scc with vertical error bars for a few selected points. Seen in this figure is a noticeable peak in the 4–6 scc range for temperatures 8 K or higher with the peak value exceeding 3.

From the limited number of adsorption isotherms measured, we calculated the isosteric heat of adsorption Q_{st}, which is given by

$$\frac{Q_{st}}{k_B} = -\left(\frac{\partial \ln P}{\partial(1/T)}\right)_{N,A} \tag{2}$$

at constant coverage N and surface area of the adsorbate A.

The measured isotherms were smoothed, and constant coverage values of P were determined as a function of $1/T$. The slopes were then calculated numerically. The results of this calculation are shown in Fig. 9. The graph also shows the isosteric heat measured by Huff and Dash[19] for Ne adsorbed on Grafoil, the calculated single atom (Ne) binding

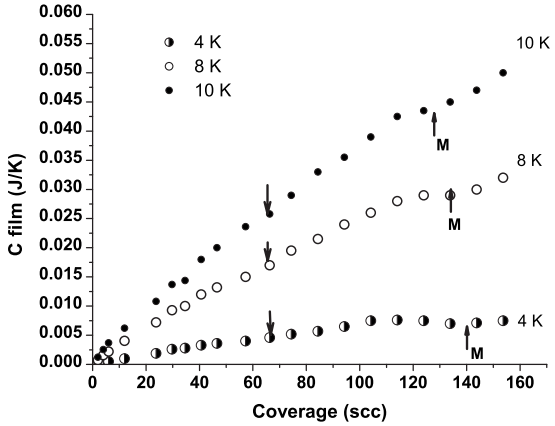

FIG. 6. Heat-capacity isotherms at select temperatures for Ne film on SWNTB. The upward arrow marked M shows monolayer completion. Downward arrow points to a feature close to three-line phase completion.

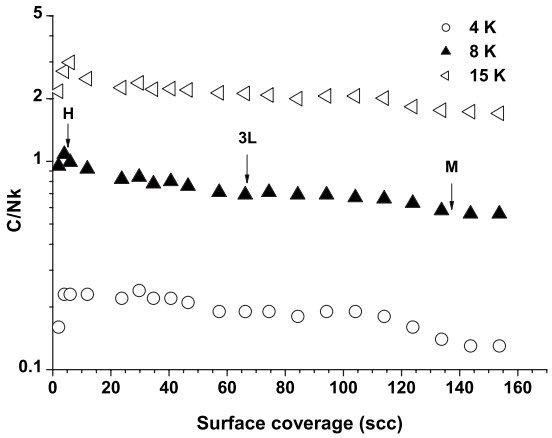

FIG. 7. Specific heat isotherm for different coverages of Ne adsorbed on SWNTB. Arrows are shown pointing to coverage corresponding to (H) heterogeneous sites completion, (3L) three-line completion, and (M) monolayer completion.

energy on Grafoil, and the heat of sublimation of 3D Ne at its triple point. In order to compare the results from this work with the measurements of Huff and Dash on Grafoil, we have set the zero coverage on Grafoil at 64 scc for our cell (see Fig. 7). Also, the monolayer completion on Grafoil was normalized to our monolayer completion at ≈135 scc. The isosteric heat starts at a rather high value of 700 K as the irregular interstitials and grooves are being occupied. This value is close to 1.8 times the isosteric heat for Ne on graphite at the limit of zero coverage. The very high binding region is followed by a broad "peak" centered at 30 scc corresponding to the region where the three-line phase is expected to be formed. As the curved surface of the carbon nanotube is occupied, the isosteric heat gradually decreases from 440 to 390 K between 60 and 110 scc. At the completion of a monolayer, the isosteric heat is 331 K. About 25 scc past the monolayer, at 160 scc, the isosteric heat is 278 K, higher than the heat of sublimation of bulk Ne at its triple point, 250 K. Notice that the Ne on Grafoil isosteric heat has a peak near monolayer coverage due to the compression of 2D fluid Ne and the crossing of the 2D melting line. We see no such contribution for Ne/SWNTB.

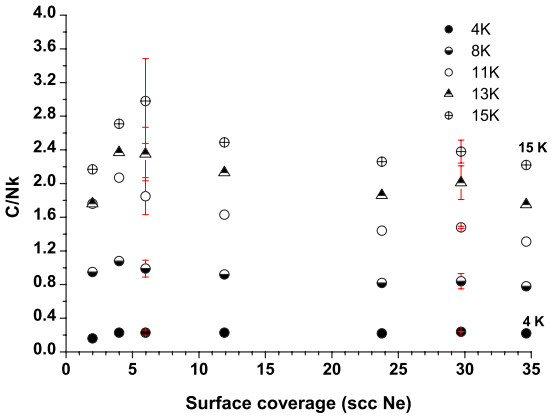

FIG. 8. (Color online) Specific heat isotherm up to 34.6 scc of Ne adsorbed on SWNTB. Estimated vertical error bars are shown for some of the data points.

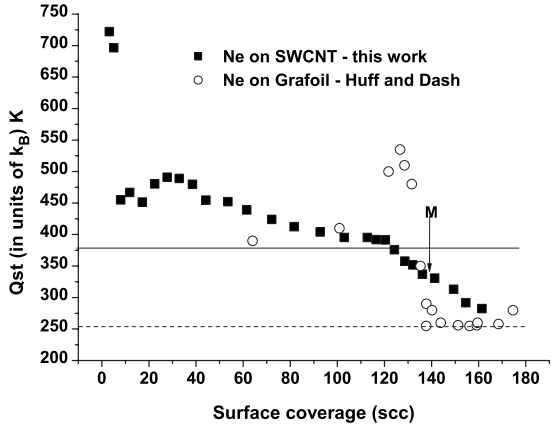

FIG. 9. Isosteric heat calculated from pressure isotherm data for Ne adsorbed on SWNTB (filled squares). Monolayer is indicated with an arrow marked M. Open circles are the isosteric heat of first layer Ne adsorbed on Grafoil (Ref. 19) scaled as described in the text. The broken line at 255 K is the latent heat of sublimation for bulk Ne at its triple point, and the solid line at 378 K is the depth of the laterally averaged potential (Ref. 39) for Ne adsorbed on graphite.

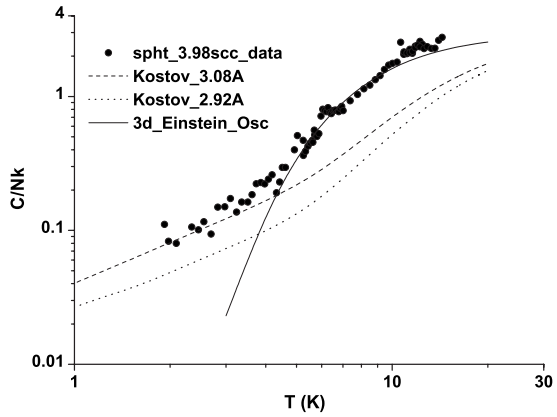

FIG. 10. Log-log plot of measured specific heat for 3.98 scc Ne film vs temperature (solid circles). Also shown are results for the model of Kostov *et al.* with 3.08 Å (dashed line) and 2.92 Å (dotted line) Ne-Ne separations and for a 3D Einstein model (solid line) with characteristic temperature of 28 K, see text.

V. ANALYSIS AND DISCUSSION

Looking at Figs. 6–9, we can identify four coverage regions for the data obtained: (1) very low coverage, perhaps below 4 to 6 scc, where the Ne atoms are coating very high binding energy sites, with Q_{st}/k_B larger than 700 K; (2) between 6 and 64 scc, a region with Q_{st}, on the average, about 1.4 times larger than the single Ne atom binding on graphite (this region should correspond to the filling of grooves from one up to three lines of Ne atoms); (3) the region between 64 and 135 scc where the outside surface of the bundles is filled with a quasi-2D layer that has many similarities with Ne/graphite (as discussed below) but without any measurable signal of a first or higher order phase transition; and (4) above 135 scc formation of the second layer.

A. Lowest densities: Crossover from one to three dimensions?

The Q_{st} calculation (in units of k_B) shown in Fig. 9 shows a couple of points at high values followed by a sharp drop. Very high values of Q_{st} followed by a drop in Q_{st} at very low coverage have been observed by Wilson and Vilches[40] for ^{4}He adsorbed on the same nanotubes and occur for a variety of isotherms on different SWNTBs.[10] This is indicative of adsorption in the highest binding energy sites and perhaps in the heterogeneous sites that are available.[10]

In this coverage region, the measured heat capacity of film plus background is barely above the background and, consequently, the film data have a very large amount of scatter. This makes precise analysis difficult. The specific heat grows rapidly and saturates to a value around and above $C/Nk \approx 2.8$ for $T > 14$ K; see Figs. 3 and 7. This is the region that leads to the peak in specific heat isotherms of Figs. 7 and 8. The high T specific heat would seem indicative of the formation of 3D clusters, except for the lowest T specific heat temperature dependence becoming closer to linear rather than cubic. A linear specific heat would be indicative of 1D solid chains. This is also the coverage region where neutron scattering from ^{4}He on very similar SWNTBs done by Pearce *et al.*[37] at about 2 K shows a reciprocal lattice vector corresponding to compressed solid linear chains of ^{4}He atoms, but remarkably with a very slightly larger average 1D lattice spacing with increasing coverage.

In Sec. II, we noted that Kostov *et al.* have calculated the phonon specific heat of Ne in a groove between two (10,10) nanotubes. Figure 10 shows the measured specific heat for 3.98 scc coverage and the specific heat for the Kostov *et al.* model for their two Ne-Ne distances. We have included in the figure the exact specific heat for the 3D Einstein model. As noted in Sec. II, Lasjaunias *et al.* fitted their very low density ^{4}He data to a 1D Einstein model. The characteristic temperature which fits our data best at high T is 28 K. The exponential behavior does not fit the data below 5 K, but this is also where the subtraction of the background is very important. At the low T end of our measurements, the film heat capacity (C_{film}) is only 10% larger than the background heat capacity, with a large random error of about 20% of C_{film}. With this uncertainity, it is interesting to note that between 2 and 4 K, the measured specific heat and the calculated specific heat using Kostov *et al.* for a linear chain of Ne atoms with $a_{\text{Ne-Ne}}=3.08$ Å are of the same order of magnitude as the measured specific heat without adjustable parameters. If we accept that the data below 4 K are in agreement with the model of Kostov *et al.*, a 1D Debye temperature of ≈ 58 K may be obtained from the measured data. The model of Kostov *et al.* in the high T limit has $C/Nk \approx 2.8$ at 60 K, a temperature much higher than that in our experiment and at which almost all Ne would be desorbed given our experimental setup. Nevertheless, as Fig. 10 shows, the shape of the calculated specific heat is similar to the shape of the measured one (emphasized by the log-log scale), shifted in T by a variable amount. This large shift could be due to the fact that the nanotubes in our bundles have 1.1 nm diameter and 1.4 nm separation between the nanotubes, rather than the 1.36 nm nanotubes with 1.7 nm separation used by Kostov *et*

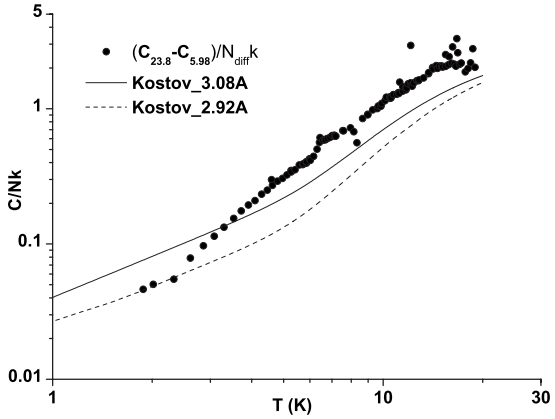

FIG. 11. Log-log plot of the difference specific heat between 23.8 scc film and a 5.98 scc film of Ne (solid circles). Also shown are results from the model of Kostov *et al.* with 3.08 and 2.92 Å Ne-Ne separations.

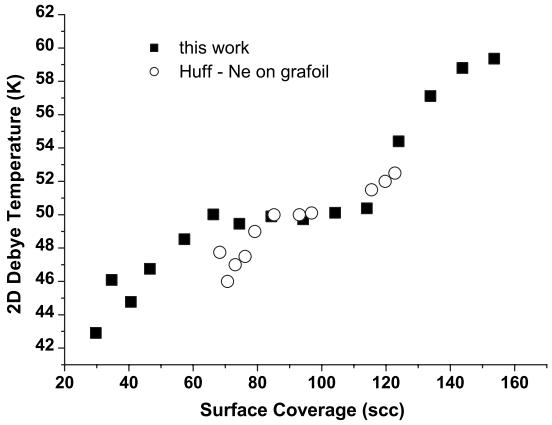

FIG. 12. 2D Debye temperature of adsorbed Ne films at several coverages. Coverages of Huff and Dash are altered to overlap the presently studied range of coverage (see text).

al. The shallower grooves in our bundles may induce the onset of the transverse modes of oscillation of the Ne chains in the grooves at a lower temperature. On the other hand, the behavior of C/Nk vs T may be due to peculiarities of the heterogeneous sites where adsorption may occur.

Finally, a small bump is barely visible in the heat-capacity data of Fig. 10 between 5 and 7 K. This feature is present in almost all the runs, up to and above monolayer completion. We will discuss it in detail in the last section.

B. Grooves and three-line region

It is important to note that in bundles with 1.1 nm nanotubes, the maximum number of lines of Ne atoms that can be placed between grooves is about 6. With our monolayer completion at roughly 135 scc, starting the dosing as going into grooves (albeit high binding grooves), then one line should be completed by about 22.5 scc and three lines by 67.5 scc. On the other hand, if we assign nearly 6 scc to independent high energy binding sites, we obtain about 21.5 scc/line of atoms on the grooves and one line of atoms would complete at ≈27 scc. The three-line phase should complete around 67–71 scc total dosing. We can see in Fig. 7 that the specific heat isotherms have a slight step down between 45 and 65 scc, especially visible at low T. The isosteric heat (see Fig. 9) though, measured at higher T, decreases smoothly, showing no evidence of completion of a "phase."

The low temperature (<9 K) specific heat versus temperature data have a component with a quadratic T dependence at all coverages above 24 scc, and there is no dramatic change in the shape of the heat capacity on completing one or three lines of atoms. Thus, the one-line or three-line coverages or phases are not well defined. We discuss the quadratic temperature dependence in detail in the next section.

Since all Ne atoms contribute to a heat-capacity measurement, and the very low density Ne may contribute a high specific heat to the total, we have looked at two coverages, 23.8 and 57.3 scc, after subtracting the smoothed measured 5.98 scc data. We show in Fig. 11 the difference specific heat $(C_{24}-C_6)/N_{diff}k_B$ data (where N_{diff} is the difference in coverage with reference to 5.98 scc), as well as the calculation of Kostov *et al.* for their two spacings. While our data again do not agree quantitatively with the model, it seems as if the measured data tend to the results of the model for a compressed 1D solid at the low T end of our measurements. It would be important to extend our measurements to much lower T to see if a linear specific heat is observed.

Kostov *et al.* did not calculate the specific heat of the three-line phase of Ne, but they presented results for this phase in CH_4. The model results for CH_4 for the three-line phase and the one-line phase are almost identical, with a linear heat capacity at the lowest T. Our 57.3 scc specific heat data with and without subtraction of the 5.98 scc run do not show any agreement with the 1D model of Kostov *et al.* We conclude that it is unlikely that the model and our results at what should be the coverage of the three-line phase will show agreement, since by 64 scc, the low T heat capacity has a quadratic dependence on T.

C. Adsorption on the curved graphene

As mentioned above, for coverages above 24 scc, the low temperature dependence of the specific heat is quadratic. Such low temperature dependence suggests a 2D Debye solid behavior. The Debye model assumes that the transverse and longitudinal modes have the same velocity and that the dispersion relation is linear. The Debye temperatures Θ_D derived from fitting the experimental data to a quadratic fit in the temperature range 2–4 K are shown in Fig. 12. The Debye temperature increases between 30 and 75 scc and stays constant at 50 K up to 105 scc before continuing to rise at still higher coverage and flattening above our 135 scc dosing. The 2D Debye temperatures extracted show qualitative and quantitative agreement with measurements[19] of Huff and Dash for 2D Ne on Grafoil. In Fig. 12, we set 64 scc in our cell as the "zero" coverage in the Ne/Grafoil experiment (somewhat arbitrarily, but it is approximately the end of the three-line phase) and 135 scc as a complete monolayer. We could get essentially perfect agreement between the Ne/SWNTB and Ne/Grafoil measurements if we ignore the

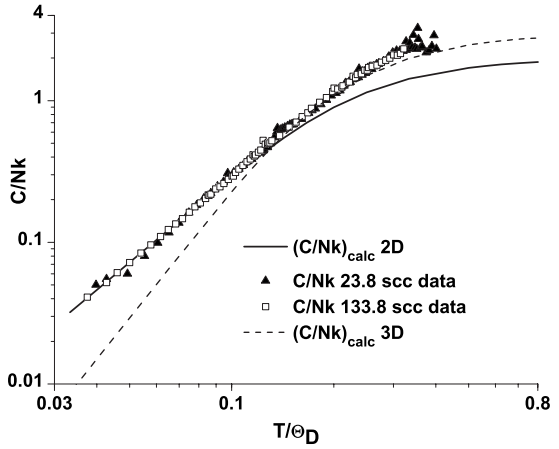

FIG. 13. Measured specific heat plotted as a function of reduced temperature for 23.8 and 133.8 scc Ne. The log-log plot also shows the specific heat calculated by solving the integrals numerically for a 2D and 3D Debye solid.

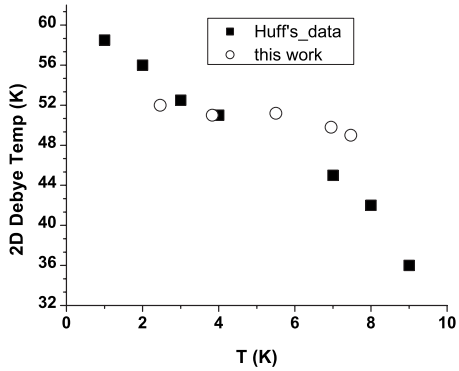

FIG. 14. 2D Debye temperatures for Ne on Grafoil (1–10 K) and on carbon nanotube bundles (2–8 K).

three-line phase and superimpose the lowest coverage of Huff and Dash with our measurements at ≈45 scc. The plateau at $\Theta_D \cong 50$ K in the measurement of Huff and Dash corresponds to the 2D solid-vapor coexistence region of Ne/graphite, where the Ne-Ne distance is constant. The increase in Θ_D in the graphite measurements above the coexistence region is due to compression of the 2D Ne. It seems like a similar effect occurs in the nanotube bundles, although we do not observe a solid melting peak. The flat Θ_D at 50 K in our results corresponds to filling of the curved graphene surface with about three lines of quasi-2D Ne, but obviously this system is more complex than Ne/graphite.

While the low temperature specific heat shows a T^2 dependence, it deviates significantly from the Debye model for temperatures greater than 0.12 Θ_D. Figure 13 shows the measured specific heats at two coverages (beginning of three lines and completion of a monolayer) plotted against the reduced temperature, which is the ratio of T/Θ_D, determined as explained in the previous paragraph. The plot also shows exact results for the specific heat of a 2D and a 3D Debye solid.

Our measured data follow the quadratic trend up to 9 K, where it rises faster than the 2D Debye model. The specific heat values at the highest temperatures measured are higher than the asymptotic limiting value of 2 for a 2D solid, although this includes remnants of the very high specific heat of the initial coverages (and all the previous coverages). As one would notice, the specific heat rises even faster than a 3D Debye solid model above 0.3 Θ_D.

Ne/Grafoil, strictly speaking, does not follow a Debye model with a single Θ_D. Huff calculated Debye temperatures at different temperature points between 1 and 10 K for a constant fractional coverage of 0.47 monolayer. He found that Θ_D decreased as the temperature increased. In Fig. 14, we reproduce Huff's Debye temperature data and our data for a total coverage of 94.2 scc, which is roughly the same fraction (0.47) of the coverage on the curved graphene surface $[0.47 \times (135-64)\ \text{scc} = 33\ \text{scc}]$ above the three-line phase (64 scc). We determined the Debye temperature at different temperature intervals, roughly 1 K wide, by plotting the measured specific heat versus a "family" of reduced temperatures. Such a family of curves was then overlapped with the exact calculation, and a Debye temperature value was chosen for a given temperature interval where there is agreement between the measured specific heat and the exact calculation. Our data also share some of the features as on Grafoil, but the effect is less pronounced. The Debye temperature shows a gradual decrease both on the higher and lower side of the 4–6 K temperature range. While we have no explanation for this difference in the Θ_D vs temperature behavior, Huff's determination of the Θ_D for a film with fractional coverage of 0.47 was carried out in the solid-vapor coexistence region. In this region, as the temperature increases from 1 to 10 K, the amount of 2D solid phase decreases whereas the 2D vapor phase increases, applying the lever rule. For the film on carbon nanotubes, the film seems to be a single-phase 2D solid.

Referring to Fig. 9, Huff and Dash[19] measured an isosteric heat for Ne/Grafoil of 410 K at about half a monolayer, followed by a sharp increase to 550 K near monolayer coverage and a sharp drop to 300 K just past the monolayer. Their Q_{st} values were based on pressure isotherms between 19.5 to 25.6 K covering the single-phase fluid, the solid-liquid coexistence, and the pure 2D solid regions of the Ne/Grafoil phase diagram. When the isosteric heat measurement on Grafoil is compared to the phase diagram determined by Rapp *et al.*,[20] the peak can be attributed to the compression of the fluid and eventually the latent heat of fusion. It is interesting to see a markedly different behavior for Ne on SWNTB. Not only is the dramatic increase absent approaching the monolayer completion, the isosteric heat at the peak coverage for Ne/Grafoil is as much as 150 K higher than on SWNTB. This may be indicative that on the narrow and long graphene surface, Ne cannot make a compressible fluid 2D phase; rather, it grows out of the grooves directly as a solid.

D. Monolayer completion and above

The completion of the monolayer is signaled by a change of slope in the heat-capacity isotherms, indicated by an M in Fig. 6 and is also noted in Figs. 7 and 9. In Ne, ^{4}He, and H_2 adsorbed on flat graphite, a compressible 2D incommensu-

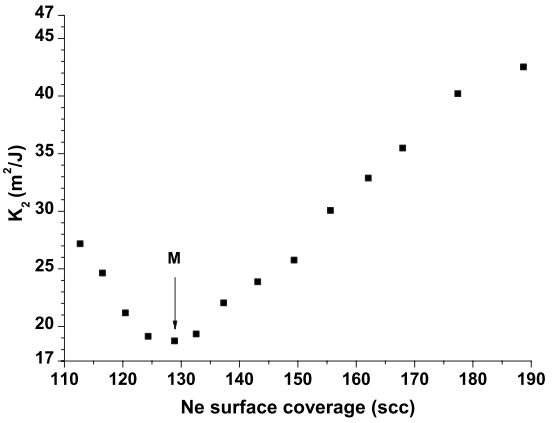

FIG. 15. Isothermal compressibility of the 2D Ne film in m^2/J at 19.2 K around monolayer coverage. Monolayer completion (marked M) is indicated by an arrow.

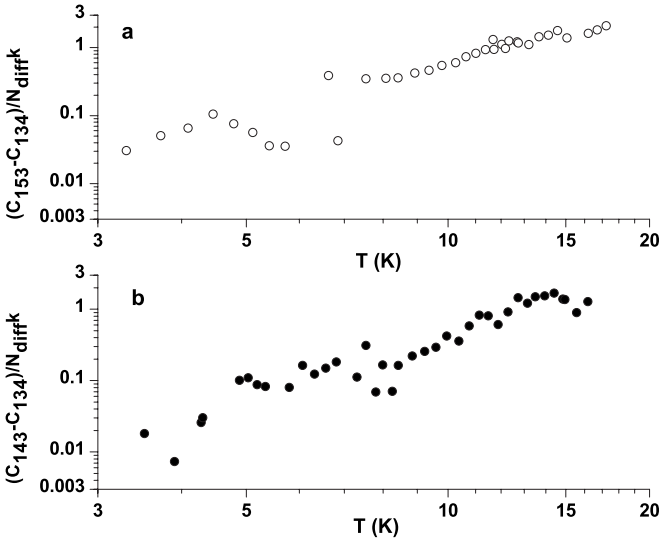

FIG. 16. Log-log plot of difference specific heat for films in the second layer in terms of number of atoms in excess of a coverage (133.8 scc) closest to monolayer (≈135 scc) vs T in the 3–20 K range. (a) 153.6–133.8 scc and (b) 143.7–133.8 scc. One negative difference data point from (a) and four from (b) were deleted when plotted in log scale. Log-log plot exaggerates scatter at the smallest specific heat.

rate solid is formed near monolayer completion. Addition of atoms and/or molecules to the surface compresses the 2D solid, increasing its Debye temperature. In ^{4}He/graphite and H_2/graphite, this compression results in a sharp minimum in heat-capacity isotherms because when a second layer begins to form, this second layer is highly mobile (a 2D gas) and has a very large specific heat compared to the first layer solid specific heat "background." For Ne/graphite, the compressibility is not as high as for the more quantum substances and there is no pronounced minimum, but the rate of increase of the heat capacity with addition of Ne becomes smaller than in the solid-vapor coexistence region. For Ne/SWNTB, we observe both the decrease in the rate of growth of C_{film}, Fig. 6, above 120 scc adsorbed and the increase after monolayer completion.

In addition to the heat-capacity isotherms, evidence for the monolayer completion comes from the compressibility of the 2D film derived from our measured vapor pressure isotherms. Figure 15 shows the 2D compressibility[41] calculated at 19.2 K. To calculate the compressibility, a specific area of 650 m^2/g was used. The compressibility attains a minimum at roughly 129 scc before continuing to rise as the surface coverage increases. This coverage corresponds to the most compressed first layer solid, the shallow minimum indicating that the second layer solid compresses some of the atoms into the first layer as coverage increases. Note that in the 10 K heat-capacity isotherms of Fig. 6, monolayer completion has already decreased to under 130 scc from the 135 scc at the lowest temperatures.

The second layer of Ne has been studied by Talapatra *et al.*[18] on (10,10) SWNTB and by Krungleviciute *et al.*[34] on HiPCo™ nanotubes who concluded that on the completed first Ne layer groove, a phase with "one line" of atoms is formed at about 1.4 monolayer coverage. Their vapor pressure isotherm measurements yield isosteric heat for this second layer groove phase of 278 K.[34] This is the same as the measurement of Q_{st} in our cell for the second layer groove phase coverages that we estimate to be around 160 scc.

In order to look for evidence of a one-line phase of atoms formed on the second layer groove, we subtracted the 133.8 scc smoothed heat capacity from the data taken at 143.7 and 153.6 scc. The results are shown in Fig. 16, where the specific heat is plotted for the atoms in excess of the monolayer coverage. The data displayed have considerable scatter because the heat-capacity minimum at monolayer completion is very shallow. Furthermore, monolayer completion may not be at 133.8 scc, and monolayer capacity is certainly smaller at 19 K (see Fig. 15) than up to 10 K, Fig. 6. With these caveats, Fig. 16 shows that below 10 K, the specific heat seems to grow toward a plateau at C/Nk between 0.2 and 0.4 before increasing rapidly between 10 and 20 K. This last increase must be due to promotion of atoms from the first layer to the second layer (groove), as well as the onset of normal and transverse excitations within the second layer "line." If this is what happens, our data would indicate that a truly 1D groove phase will form only below 10 K. We do not have specific heat data at 1.4 monolayer to compare directly to the work referenced above.[34]

E. Small peak in the heat capacity at 6–7 K

There is a small feature in the film heat capacity in the 6–7 K range, shown in Fig. 17 for three selected coverages (29.7, 46.6, and 94.2 scc). The temperature at which the peak occurs increases very slowly with coverage, being centered at ≈7 K for 153.6 scc coverage. Figure 18 is the heat-capacity difference between the actual film heat-capacity data and a smooth fit under the peak. The area under the peak is ≈0.35 mJ. The area under the peak stays essentially constant regardless of the surface coverage and is seen even when the heterogeneous sites and grooves are being populated (see Fig. 10), during three-line phase formation and when Ne occupies the curved graphene surface. Also shown in Fig. 18 is the scatter in the data for the corresponding

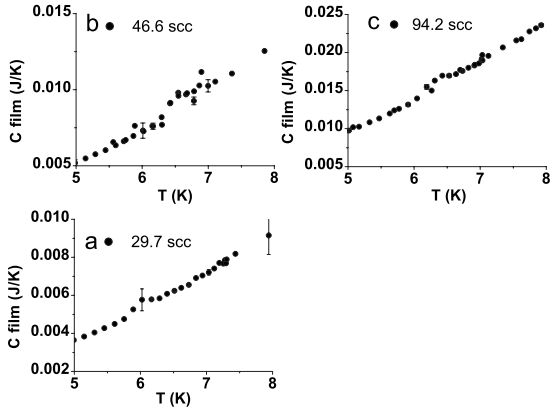

FIG. 17. Heat capacity between 5 and 8 K showing a feature in the heat capacity at around 6.5 K. Heat capacity for (a) 29.7 scc, (b) 46.6 scc, and (c) 94.2 scc Ne films. Error bars are shown for the film heat capacity.

background. The small scatter for the same temperature range indicates that the observed feature in the film heat capacity is not due to any anomaly in the background heat capacity.

We do not have an interpretation for this feature. It clearly seems to be a property of the very initial stages of Ne adsorption, appearing on two completely independent data runs, each one with its own background measurement. The small shift in average temperature is reminiscent of compression of a solid. For reference, the latent heat associated with triple point melting of Ne/Grafoil is ≈1.7 mJ/scc (Ref. 42) adsorbed, while it is ≈5.1 mJ/scc (Ref. 43) for Ne adsorbed on graphite foam. Thus, if anything similar was going on here, it would happen within the first 0.2 scc or so adsorbed, ten times lower coverage than our lowest measurement.

VI. SUMMARY AND CONCLUSIONS

We have measured the heat capacity of Ne films adsorbed on HiPCo single-wall carbon nanotube bundles of average tube diameter of 1.1 nm, between 0.015 and 1.19 monolayers, and for a temperature range from 2 to 19 K, complemented by volumetric adsorption isotherm measurements above 18 K. Monolayer completion, for our calorimeter cell, is at about 135 scc. This range of coverages and temperatures has given us a qualitative and semiquantitative understanding of possible regions, not necessarily phases, formed in the first Ne layer as a function of amount of Ne adsorbed.

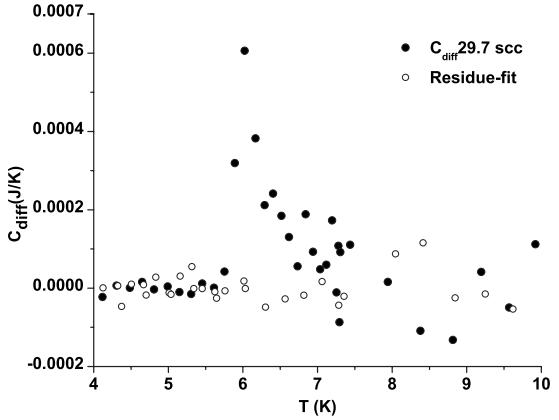

FIG. 18. Difference heat capacity (as explained in the text) between 4 and 10 K showing a feature in the heat capacity at around 6.5 K. Also shown on the same plot is the difference between background heat-capacity data and a smooth fit to the background.

We observe a very small peak (or feature) in the heat capacity at all coverages measured, which is due to the gas adsorbed. It is located between 5 and 7 K, with a slightly increasing T_{peak} with increasing coverage. Its magnitude does not change with coverage, but the feature is not in the background calorimeter heat capacity. We believe that it is due to Ne in some very high binding energy sites, and we estimate the dosing needed to produce it to be at least ten times smaller than the smallest dose we measured. We cannot say more about it, but the extremely low coverage heat capacity of any gas on relatively uniform Grafoil also shows very low coverage peculiarities due to adsorption on very heterogeneous sites. We have ignored this feature in the general analysis.

At very low coverages, below 4% of a monolayer, the atoms populate high binding sites. The isosteric heat is 700 K or higher. This value is consistent with the calculated zero temperature single particle binding energy of 659 K (Ref. 27) for the groove sites and higher than the measured binding energies of first layer Ne on the 1D groove sites of carbon nanotubes (602 K).[17] Specific heat isotherms show a "maximum" centered at 4–6 scc, clearly visible as a peak at 6 scc coverage at $T > 11$ K. In this very low coverage region, Ne could form linear chains, likely of nonuniform density. The measured heat capacity has some characteristics resembling a model developed by Kostov *et al.*, but only qualitatively. Measurements of the lattice spacing between the Ne atoms and identification of possible linear chains would be highly desirable.

Increasing the coverage, the isosteric heat (determined between 17 and 28 K) shows a very rounded maximum roughly between 12 and 60 scc, with average value of $Q_{st}/k_B \approx 450-460$ K, with a height of 40 K at 30 scc. This is the region where theoretical models expect Ne to form one line and three lines of atoms, in succession, anchored by grooves between two nanotubes on the outside of the bundles. We have looked for specific features in the heat-capacity data over this region, but it looks as if the film grows smoothly from the initial high binding sites without showing sharp boundaries. While at 24 scc adsorbed the lowest T heat capacity may become linear in T, the behavior smoothly changes to a T^2 low temperature dependence with increasing coverage. In this region, it would be particularly useful to extend the heat-capacity measurements to below 1 K to observe the film's temperature dependence.

For coverages approximately between 65 and 135 scc, Ne completes occupying the outside graphene surface of the bundle. For our nanotubes, only about six lines of Ne atoms can be formed between contiguous grooves; thus, roughly from 65 scc onward, half the Ne atoms are in the grooves and two adjacent lines and the rest start to coat the outside surface of the bundle surface nanotubes. These films appear

to be two dimensional at low T, in the sense that the heat capacity has a T^2 dependence. Debye temperatures extracted from the low T tails agree remarkably well with the ones calculated on flat graphite for similar densities. The relatively high T isosteric heat in this region of coverage is comparable to the one on flat graphite, but we do not observe the peak in Q_{st} observed on Ne/graphite, which is due to compression of a fluid monolayer and the latent heat of 2D melting. The high T limit of the specific heat, though, may be higher than 2, but this is uncertain because we do not know how to identify that portion of the film that is strictly two dimensional, and on the curved surface and grooves, some characteristics of these films may be three dimensional. For Ne/graphite, the low T 2D solid melts at a spectacular triple point located at 13.5 K. We searched for even remnants of this feature and did not find any. In fact, extrapolation of our heat-capacity measurements to $T=0$ K and then integration of C/T vs T up to 18 K yield less entropy than for the 2D Ne/graphite case. How the melting of these narrow 2D stripes occurs, if it happens at all before desorption sets in, should be an interesting topic to pursue.

An inflection in heat-capacity isotherms, or a drop in the specific heat isotherms, and a minimum in the 2D compressibility at 19 K signify the completion of the monolayer. This behavior is also very similar to the one of Ne/graphite. Again, in this region, it would be very interesting to do diffraction measurements to obtain the lattice spacing of the adsorbate.

ACKNOWLEDGMENTS

We thank J. G. Dash, D. B. Pengra, M. P. den Nijs, and D. H. Cobden for helpful discussions during the writing of this paper and D. Rammunno-Johnson for developing the initial version of the program in LabView for heat-capacity measurement. We thank M. W. Cole, M. K. Kostov, A. D. Migone, and V. Krungleviciute for many informal discussions of our results. We wish to thank the NSF for Grants No. DMR 0245423 and No. 0606078 and the Bosack-Kruger Foundation for partial support of this research.

*Author to whom correspondence should be addressed; lowtemp@u.washington.edu

[1] L. W. Bruch, M. W. Cole, and E. Zaremba, *Physical Adsorption: Forces and Phenomena* (Clarendon, Oxford, 1997).
[2] M. Bretz, J. G. Dash, D. C. Hickernell, E. O. McLean, and O. E. Vilches, Phys. Rev. A **8**, 1589 (1973).
[3] R. L. Elgin and D. L. Goodstein, Phys. Rev. A **9**, 2657 (1974).
[4] R. E. Ecke, Q.-S. Shu, T. S. Sullivan, and O. E. Vilches, Phys. Rev. B **31**, 448 (1985).
[5] D. S. Greywall, Phys. Rev. B **47**, 309 (1993).
[6] F. C. Motteler and J. G. Dash, Phys. Rev. B **31**, 346 (1985).
[7] M. E. Pierce and E. Manousakis, Phys. Rev. B **62**, 5228 (2000).
[8] E. V. L. de Mello and G. M. Carneiro, Surf. Sci. **169**, 357 (1986).
[9] M. J. Tejwani, O. Ferreira, and O. E. Vilches, Phys. Rev. Lett. **44**, 152 (1980).
[10] W. Shi and J. K. Johnson, Phys. Rev. Lett. **91**, 015504 (2003).
[11] G. Stan, M. J. Bojan, S. Curtarolo, S. M. Gatica, and M. W. Cole, Phys. Rev. B **62**, 2173 (2000).
[12] R. E. Peierls, Ann. Inst. Henri Poincare **5**, 177 (1935).
[13] J. K. Percus, Mol. Phys. **100**, 2417 (2002).
[14] L. D. Landau and E. M. Lifshitz, *Statistical Physics* (Pergamon, New York, 1958).
[15] J. M. Phillips and J. G. Dash, J. Stat. Phys. **120**, 721 (2005).
[16] M. M. Calbi, M. W. Cole, S. M. Gatica, M. J. Bojan, and G. Stan, Rev. Mod. Phys. **73**, 857 (2001).
[17] S. Talapatra, A. Z. Zambano, S. E. Weber, and A. D. Migone, Phys. Rev. Lett. **85**, 138 (2000).
[18] S. Talapatra, V. Krungleviciute, and A. D. Migone, Phys. Rev. Lett. **89**, 246106 (2002).
[19] G. B. Huff and J. G. Dash, J. Low Temp. Phys. **24**, 155 (1976).
[20] R. E. Rapp, E. P. de Souza, and E. Lerner, Phys. Rev. B **24**, 2196 (1981).
[21] D. B. Pengra and J. G. Dash, J. Phys.: Condens. Matter **4**, 7317 (1992).
[22] C. Tiby, H. Wiechert, and H. Lauter, Surf. Sci. **119**, 21 (1982).
[23] S. Calisti and J. Suzanne, Surf. Sci. **105**, L255 (1981).
[24] S. Calisti, J. Suzanne, and J. A. Venables, Surf. Sci. **115**, 455 (1982).
[25] M. M. Calbi and M. W. Cole, Phys. Rev. B **66**, 115413 (2002).
[26] G. Vidali, G. Ihm, H. Y. Kim, and M. W. Cole, Surf. Sci. Rep. **12**, 135 (1991).
[27] M. C. Gordillo, L. Brualla, and S. Fantoni, Phys. Rev. B **70**, 245420 (2004).
[28] M. M. Calbi and J. L. Riccardo, Phys. Rev. Lett. **94**, 246103 (2005).
[29] M. K. Kostov, M. M. Calbi, and M. W. Cole, Phys. Rev. B **68**, 245403 (2003).
[30] C. Journet, W. K. Maser, P. Bernier, A. Loiseau, M. L. dela Chapelle, S. Lefrant, P. Deniard, R. Lee, and J. E. Fisher, Nature (London) **388**, 756 (1997).
[31] S. L. Fang, A. M. Rao, P. C. Eklund, P. Nikolaev, A. G. Rinzler, and R. E. Smalley, J. Mater. Res. **13**, 2405 (1998).
[32] S. Rols, R. Almairac, L. Henrard, E. Anglaret, and J.-L. Sauvajol, Eur. Phys. J. B **10**, 263 (1999).
[33] M. Bienfait, P. Zeppenfeld, N. Dupont-Pavlovsky, M. Muris, M. R. Johnson, T. Wilson, M. DePies, and O. E. Vilches, Phys. Rev. B **70**, 035410 (2004).
[34] V. Krungleviciute, L. Heroux, S. Talapatra, and A. D. Migone, Nano Lett. **4**, 1133 (2004).
[35] J. C. Lasjaunias, K. Biljaković, J.-L. Sauvajol, and P. Monceau, Phys. Rev. Lett. **91**, 025901 (2003).
[36] T. A. Wilson, Ph.D. thesis, University of Washington, 2004.
[37] J. V. Pearce, M. A. Adams, O. E. Vilches, M. R. Johnson, and H. R. Glyde, Phys. Rev. Lett. **95**, 185302 (2005).
[38] D. M. Young and A. D. Crowell, *Physical Adsorption of Gases* (Butterworths, London, 1962).
[39] G. Vidali and M. W. Cole, Phys. Rev. B **29**, 6736 (1984).
[40] T. A. Wilson and O. E. Vilches, Physica B **329-333**, 278 (2003).
[41] J. G. Dash, *Films on Solid Surfaces* (Academic, New York, 1975).
[42] G. B. Huff, Ph.D. thesis, University of Washington, 1972.
[43] D. B. Pengra, Ph.D. thesis, University of Washington, 1991.